CLASSIFICATION cancelled

NACA

RESEARCH MEMORANDUM

AERODYNAMIC CHARACTERISTICS OF A CIRCULAR CYLINDER

AT MACH NUMBER 6.86 AND ANGLES

OF ATTACK UP TO 90°

By Jim A. Penland

Langley Aeronautical Laboratory
Langley Field, Va.

NATIONAL ADVISORY COMMITTEE
FOR AERONAUTICS

WASHINGTON
March 11, 1954

CLASSIFICATION cancelled

NATIONAL ADVISORY COMMITTEE FOR AERONAUTICS

RESEARCH MEMORANDUM

AERODYNAMIC CHARACTERISTICS OF A CIRCULAR CYLINDER

AT MACH NUMBER 6.86 AND ANGLES

OF ATTACK UP TO 90°

By Jim A. Penland

SUMMARY

Pressure-distribution and force tests of a circular cylinder have been made in the Langley 11-inch hypersonic tunnel at a Mach number of 6.86, a Reynolds number of 129,000 based on diameter, and angles of attack up to 90°. The results are compared with the hypersonic approximation of Grimminger, Williams, and Young and with a simple modification of the Newtonian flow theory. The comparison of experimental results shows that either theory gives adequate general aerodynamic characteristics but that the modified Newtonian theory gives a more accurate prediction of the pressure distribution. The calculated crossflow drag coefficients plotted as a function of crossflow Mach number were found to be in reasonable agreement with similar results obtained from other investigations at lower supersonic Mach numbers. Comparison of the results of this investigation with data obtained at a lower Mach number indicates that the drag coefficient of a cylinder normal to the flow is relatively constant for Mach numbers above about 4.

INTRODUCTION

Recently, it has become evident that a missile returning to the earth's surface at a high supersonic speed from a flight at extreme altitudes may reenter the atmosphere at a very high angle of attack or may possibly be tumbling end over end. Such conditions of flight could impose severe aerodynamic loads on the structure. The various forces on a missile in all possible flight attitudes are therefore important from a structural standpoint and also for the determination of the missile's probable trajectory.

Since a large part of nearly all missiles is either cylindrical or nearly cylindrical, the aerodynamic characteristics of much of the missile

may be approximated at high angles of attack by those of a circular cylinder. Experimental aerodynamic characteristics of circular cylinders are available only up to a Mach number of about 4 (ref. 1). For higher Mach numbers, knowledge up to this time depends largely upon theory - notably, the hypersonic approximation of Grimminger, Williams, and Young (ref. 2) in which use is made of the Newtonian impact theory and the crossflow theory (ref. 3). The purpose of this investigation is to extend the range of experimental data for the circular cylinder to a Mach number of about 7 and to use the results to evaluate the theoretical methods.

SYMBOLS

d	diameter
D	drag force, measured parallel to free stream
L	lift force, measured normal to free stream
l	length of cylinder model
M	free-stream Mach number
M_c	crossflow Mach number, $M \sin \alpha$
N	normal force, measured normal to body axis
P_o	stagnation pressure
P_1	free-stream static pressure
P_3	stagnation pressure behind shock of flow component normal to shock
P_c	measured pressure on cylinder
q_1	free-stream dynamic pressure
q_c	crossflow dynamic pressure
α	angle of attack
β	radial angle about body axis measured from stagnation point

$$\frac{\Delta P}{q} = \frac{P_c - P_1}{q_1}$$

C_N normal-force coefficient of cylinder, $N/q_1 l d$

C_{D_S} drag coefficient of sphere, $4D/q_1 \pi d^2$

C_L lift coefficient of cylinder, $L/q_1 l d$

C_D drag coefficient of cylinder, $D/q_1 l d$

L/D lift-drag ratio of cylinder

$\dfrac{P_3 - P_1}{q}$ theoretical adiabatic stagnation pressure coefficient,

$$\frac{P_3/P_o - P_1/P_o}{M^2(\gamma/2)(P_1/P_o)}$$

APPARATUS

Wind tunnel.- The tests discussed in this paper were conducted in the Langley 11-inch hypersonic tunnel. This blowdown tunnel is equipped with a single-step two-dimensional nozzle designed by the method of characteristics and operates at an average Mach number of 6.86. The duration of the tunnel operating cycle for all tests was limited to approximately 70 seconds to conserve pumping time, and, because of a small variation of Mach number with time, all data used were taken at a specific time corresponding to $M = 6.86$. A detailed description of this facility may be found in reference 4.

Force models.- The force models used for lift and drag tests consisted of a series of six 1/2-inch-diameter steel cylinders, each having a projected length of 4 inches exposed to the airstream (fig. 1). The true length of these models varied from 4 inches for the $\alpha = 90^\circ$ model to 15.41 inches for the $\alpha = 15^\circ$ model. By increasing the length of the force models as the angle of attack decreased, it was possible to keep the forces high and thereby hold the accuracy of measurements more constant in order to minimize end effects. The ends of each model were machined to an angle equal to the design angle of attack of the model so that these ends would be parallel to the stream. As a check to determine the effectiveness of these oblique tips, pressure orifices were installed on the center lines of the ends of the 30° force model after force tests were completed (fig. 2). The variation of drag

coefficient with the fineness ratio of circular cylinders normal to
M = 6.86 flow was determined by making force measurements on 5/16-inch-
and 5/8-inch-diameter cylinders each having lengths of 2 and 4 inches.
In order to check further the validity of the hypersonic approximation,
a 1/2-inch-diameter steel sphere was tested at M = 6.86. All force
models were sting supported from the geometric center of each model.
The sting was attached to each cylinder model by means of a set screw
placed on the downstream side of the cylinder to shield it from the
stream. The sphere model was silver soldered to its supporting sting.

Pressure model.- The pressure model was a 1/2-inch-diameter canti-
lever steel cylinder approximately 10 inches long (fig. 3). Six
0.030-inch-diameter pressure orifices, evenly spaced radially 60° apart,
were located approximately 5 inches from the nose (fig. 4). This model
could be rotated about its longitudinal axis for locating the pressure
orifices with relation to the stream and the changes in angle of attack
were accomplished by rotating the cylinder and its conical mount about
an axis normal to the stream, parallel to the tunnel floor, and located
in the end of the sting mount. The cylinder, supported by the down-
stream end, was secured against rotation and the angle of attack of the
configuration was locked in position by set screws which may be seen in
figure 4. As on the force models the pressure model was supplied with
oblique angular tip caps to minimize tip effects by making the end
parallel to the stream direction. In addition to the oblique tip caps,
two cones of 10° and 30° angles were provided for the pressure probe to
determine the effects of the different tips.

The angles of attack for the force models and the pressure model
were preset before each test, but the angles used in analysis of data
were measured from schlieren photographs to take in consideration the
possible deflection of the models due to the aerodynamic loading.

Strain-gage force balance.- A three-component strain-gage balance
was used to measure all forces acting on the cylinder force models
described in this paper. This balance has a maximum capacity of 20 pounds
lift and 10 pounds drag, measurable to an accuracy of 0.1 pound and
0.05 pound, respectively. A more detailed description of this instru-
ment may be found in reference 5.

Pressure recorders.- Continuous records of stagnation and orifice
pressures on the cylinder pressure probe were made for all pressure
tests, and stagnation pressure was recorded during all force tests.
All pressures were measured and recorded on film by means of aneroid-
type instruments which magnify the movements of a corrugated face of
an evacuated cell. The accuracy of these instruments is ±1/2 percent
at full scale. For the present tests, instruments were selected which
had a maximum range near the expected maximum pressure to help minimize
any additional error. A more detailed description of this instrument
may be found in reference 6.

Schlieren system.- A Z-type single-pass two-mirror schlieren system was used for all tests covered in this paper. The mirrors were 12 inches in diameter with a focal length of 120 inches, and the light source was a standard A-H6 water-cooled mercury-vapor lamp. Super XX aerographic film, exposed approximately 3 microseconds and normally developed, was used for all tests. The knife edge used for varying the cutoff in the schlieren system was always placed parallel to the flow.

THEORETICAL METHODS

Hypersonic approximation.- Grimminger, Williams, and Young (ref. 2) made a series of estimates of the effect of centrifugal force on the hypersonic flow over inclined bodies of revolution and modified the theory of Newtonian flow to include these effects. The various estimates in reference 2 of the centrifugal force of the air as it traveled in a curved path around a body of revolution were based upon different body-layer stream-tube velocities. Five different relations were developed to evaluate the effective body-layer stream-tube velocity. The results of using the fifth relation show that a reasonable pressure distribution may be predicted for ogive bodies of revolution and that the drag of spheres may be accurately predicted for high Mach numbers. The theory based upon this fifth relation is subsequently referred to as Grimminger's hypersonic approximation throughout this paper.

Modified Newtonian flow.- The stagnation pressure coefficient predicted by both Newtonian flow and Grimminger's hypersonic approximation is about 10 percent higher than the theoretical adiabatic pressure coefficient for an infinite Mach number. Because of this overestimation, a modified method is presented in which the assumptions of Newtonian flow are used, namely, that when the airstream strikes a surface it loses the component of momentum normal to the surface and moves along the surface with the tangential component of momentum unchanged, except that the theoretical stagnation pressure coefficient for the Mach number of the flow being considered is substituted for the Newtonian stagnation pressure coefficient. The percentage difference between the Newtonian value and the calculated value of the pressure coefficient is then applied to the whole pressure distribution. The results predicted by this method are subsequently referred to as modified Newtonian flow.

Crossflow theory.- Another approach for approximating coefficients on inclined bodies is the crossflow theory which is essentially a variation of the well-known sweep effect. For circular wires, Jones (ref. 3) shows that the component of the drag normal to the wire may be found if the stream velocity and the angle of attack are known. The crossflow theory resolves the stream velocity into two components, one parallel

to the axis of the body and the other normal to the axis of the body.
The effective stagnation pressure and the dynamic pressure for the cross-
flow component are a function of the crossflow Mach number and the
static pressure. If the assumption is correct that the flow may be
resolved into components, then the possibility arises that low Mach
number data may be used to estimate the values of high Mach number
coefficients at angles of attack by using the low Mach number flow as
the crossflow on a body at an angle of attack in high Mach number flow.

TEST CONDITIONS

By means of a regulating valve the stagnation pressure was held to
an average value of 25.7 atmospheres. The stagnation temperature was
maintained at an average value of 668° F by means of a variable-frequency,
resistance-tube heater to ensure against liquefaction of the air. This
heater consists of a shielded group of electrically heated metal tubes
located between the high-pressure storage tank and the settling chamber
of the nozzle. The air is heated by coming in contact with the inside
walls of the metal tubes whose temperature is controlled by a variation
of the applied voltage. This air heater replaces the storage-type heat
exchanger described in reference 6. In order to make certain that there
would be no water-condensation effects, the absolute humidity was kept
less than 1.87×10^{-5} pounds of water vapor per pound of dry air for
all tests. The Reynolds number for the 11-inch hypersonic tunnel is
10,000 per inch per atmosphere stagnation pressure. The value of
Reynolds number corresponding to the stagnation pressure used for the
present tests was 257,000 per inch or 129,000 for the 1/2-inch-diameter
cylinders.

RESULTS AND DISCUSSION

Pressure-Test Results

Pressure distributions.- The variation with angle of attack of the
pressure distribution about a circular cylinder at $M = 6.86$ is pre-
sented in figure 5(a). More detail as to the point of separation and
the values of the pressure coefficient on the downstream side of the
cylinder may be seen in figure 5(b). In both measuring the pressures
and plotting the results, the assumption was made that the pressure
distribution was symmetrical about the center line of the cylinder.
The point of separation appears to vary from about 120° from the stagna-
tion point for an angle of attack of 90° to about 100° from the stagna-
tion point for an angle of attack of 14.9°. The value of pressure coef-
ficient $\Delta P/q$ at the stagnation point on the cylinder (fig. 5(a)) varies

from 1.73 for an angle of attack of 90° to 0.119 for an angle of attack
of 14.9°, and from 0.25 to -0.015, respectively, at the rearmost portion
of the cylinder. The value of the pressure coefficient for pressure
equal to zero is -0.03 and is indicated as a solid line on figure 5(b).
The pressure distributions as predicted by Newtonian flow and by
Grimminger's hypersonic approximation (ref. 2) are shown in figure 6.
It may be seen that both Newtonian theory and Grimminger's hypersonic
approximation overestimate the stagnation pressure coefficient and that
of the surrounding region. The point of zero pressure coefficient is
given as 90° from the stagnation point by both Newtonian theory and
Grimminger's hypersonic approximation, but the present tests show that
the point of zero pressure coefficient takes place at about 120° for a
cylinder normal to the flow at $M = 6.86$. The pressure distribution
predicted by modified Newtonian flow is shown in figure 6 and gives
more reasonable values of pressure coefficient in the region near the
stagnation point on the cylinder, but, as predicted by unmodified
Newtonian theory or Grimminger's hypersonic approximation, the point of
zero pressure coefficient is still given as 90° from the stagnation
point instead of the value of 120° shown by experiment. It may be seen
that the agreement between the experimental values of pressure coeffi-
cient at $\alpha = 90^\circ$ and the modified Newtonian pressure distribution is
only fair. For all other angles of attack except $\alpha = 14.9^\circ$, this
agreement was found to be much better.

Pressure model end effects.- In order to assure that the measured
pressures were not affected by the nose tips, two additional tips were
tested on the pressure model at an angle of attack of 15°. These tips
consisted of a 10° and a 30° cone. Schlieren photographs of the pressure
model with the various tips installed may be seen in figure 7. Com-
parison of the pressure distributions around this cylindrical pressure
model with the different tips installed showed that there was no
appreciable difference in the values of the measured pressures.
Although no variation was found in the pressures with different tips,
it must be noted that the shock near the orifices was not parallel to
the body surface during the $\alpha = 15^\circ$ tests. There was, however, no
measurable difference in the slope of the shock or the distance of the
shock from the surface of the model in the vicinity of the orifices for
the different tips used in the $\alpha = 15^\circ$ tests. This is an end effect
that was not present at other angles of attack. It may be seen in the
schlieren photograph (fig. 7(d)) of the pressure model during the
$\alpha = 60^\circ$ test that, in the region of the measuring station, approxi-
mately 9 diameters from the tip, the shock profile is parallel to the
model surface, an indication that no end effects from either end were
present.

Force-Test Results

Force coefficients.- The variation with angle of attack of the normal-force coefficient of a circular cylinder at $M = 6.86$ is presented in figure 8. The normal-force coefficients were determined from pressure distributions by integration and by the resolution of the lift and drag forces measured on the strain-gage balance. Experimental force measurements showed that the conical sting support used for all force models could not cause an error of more than about 1.5 percent for the force measurements, and therefore no corrections were made upon measured forces. For comparison with the experimental force and pressure data, the normal-force coefficients as predicted by Newtonian flow, Grimminger's hypersonic approximation, and the modified Newtonian flow for various angles of attack are included in figure 8. Because these theories, based upon the concept of Newtonian flow, predict only the normal-force coefficient by means of integration of the predicted pressure distributions, the skin-friction drag is not included in the theoretical curves. The theoretical curves should therefore be compared with the force coefficients obtained from pressure distributions which also do not include skin friction. It may be seen that Newtonian theory gives good predictions at low angles of attack, but at higher angles of attack the predictions are not so good, with the maximum error becoming about 10 percent at $\alpha = 90^{\circ}$. From this comparison with experimental data it appears that either Grimminger's hypersonic approximation or the modified Newtonian approximation give reasonably accurate predictions of the normal force on a circular cylinder at $M = 6.86$. It is not known whether these approximations will give equally accurate predictions for different bodies at $M = 6.86$. It may be seen in figure 9 that the drag coefficient for a sphere is overestimated at high Mach numbers by unmodified Newtonian flow but is predicted with reasonable accuracy by the hypersonic approximation and modified Newtonian flow. A comparison of the flow around a 1/2-inch-diameter sphere and a 1/2-inch-diameter circular cylinder normal to the flow may be seen in figure 10. The bow wave is seen to be much closer to the surface of the sphere than to surface of the cylinder, and the angle between the shock downstream of the model and the stream direction is appreciably smaller for the sphere than for the cylinder.

The variation with angle of attack of the lift and drag coefficients of a circular cylinder at $M = 6.86$ is presented in figure 11. It may be seen that both Grimminger's hypersonic approximation and the modified Newtonian method accurately predict the experimental lift and drag coefficients at angles of attack where the friction drag is a very small portion of the total drag. Neither of these methods take into account skin friction and both of them therefore underestimate the drag values and overestimate the values of lift-drag ratio at low angles of attack. It should be noted that the curve of lift-drag ratio is the cotangent of the angle of attack for the Newtonian flow, the

hypersonic approximation by Grimminger, and the modified Newtonian
theory. The lift-drag ratio curve in figure 11 is therefore the same
for all theories discussed in this paper. It is to be expected that
the drag coefficients obtained from pressure distributions will be
lower than those obtained from force-balance measurements because skin-
friction drag is not included in the pressure drag.

Force-model end effects.- One possible source of error in the lift
coefficients from the force tests is that the pressures on the two ends
of the cylinder might be different. Inspection of the schlieren photo-
graphs of the force models (fig. 12) shows that, as the angle of attack
is decreased, the shock patterns on the ends are very different, which
could possibly result in different pressures on the two cylinder ends.
Therfore, in order to investigate the pressures on the flat ends of the
force models, orifices were installed on the 30° force model as shown
in figure 2. The results of this test showed that there were no measur-
able differences in the pressures either between orifices or between
ends of the force model. A schlieren photograph taken during this test
may be seen in figure 12(d) and the shock formation shows no variation
from the 30° force model without pressure orifices (fig. 12(c)). It
may therefore be concluded that the flat ends did not contribute to the
lift force during the force-balance tests.

The variation with fineness ratio of the drag coefficient of a
cylinder normal to the flow at $M = 6.86$ is presented in figure 13.
The drag coefficient is seen to vary a relatively small amount and some-
what erratically as the fineness ratio varies from a value of 3 to a
value of 13. It is believed that this variation constitutes no partic-
ular trend and that the irregularity is due to scatter in the data.
From this investigation, it seems apparent that the variation of the
drag coefficient due to end effects on the cylinder normal to the flow
are small and are obscured by the scatter of the data which in this
case are within the accuracy of the apparatus involved. These results
therefore indicate that the forces measured on the cylinder models at
angle of attack are representative of forces on infinite cylinders.

Reynolds number.- The variation of fineness ratio was obtained by
varying both the length and the diameter. Each diameter therefore con-
stitutes a different Reynolds number. It may be seen in figure 13 that
there was little variation in the drag coefficients for the three
cylinders although the Reynolds number varied from about 80,400 for
the 5/16-inch-diameter cylinder to about 160,800 for the 5/8-inch-
diameter cylinder. In the Reynolds number range of this investigation
at $M = 6.86$, the effect of Reynolds number may therefore be considered
negligible for cylinders at high angles of attack.

Crossflow Results

Crossflow Mach number stagnation pressure coefficient.- The variation with crossflow Mach number of the stagnation pressure coefficient of a circular cylinder is presented in figure 14. For comparison with experimental data, a curve of theoretical stagnation pressure coefficient is included for various Mach numbers. It may be seen that the experimental stagnation pressure coefficients, obtained by crossflow theory from pressure distributions around cylinders at angle of attack in $M = 6.86$ flow, agree closely with the theoretical curve with the exception of the point at $M_c = 1.74$. It was found through close examination of the schlieren photograph of the pressure probe at $\alpha = 15^\circ$ (fig. 7) that the shock in front of the cylinder was not parallel to the surface of the cylinder in the vicinity of the orifices. The crossflow Mach number was calculated from the angle of attack of the model and the resulting pressure coefficient was high as shown in figure 14 at $M_c = 1.74$. If the crossflow Mach number is calculated from the angle of attack of the shock instead of the model, the pressure coefficient $\dfrac{P_3 - P_1}{q_c}$ then falls on the theoretical curve. This variation in stagnation pressure coefficient, due to the fact that the shock is not parallel to the body, is an end effect which appears to become significant for the present test conditions at an angle of attack of about 15° and below. Data included in figure 14 from reference 1 also show a higher-than-normal stagnation pressure coefficient at a crossflow Mach number of 1.04 which corresponds to an angle of attack of 15° in $M = 4.04$ flow. As described previously, tests indicated that there was no appreciable difference in the pressure distribution around the pressure probe whether it was supplied with a 10° cone, 30° cone, or the oblique tip. The region immediately downstream of the nose of a cone-cylinder configuration is markedly affected by the flow around the nose, but at the present test conditions the orifices were located far enough downstream to minimize this effect above an angle of attack of 15°. It is therefore apparent for the present test conditions that the stagnation pressure coefficient is not affected appreciably by the shape of the tip but is probably affected by the location of the pressure orifices in relation to the nose. It may be seen that data from references 1 and 10 for various low-supersonic crossflow Mach numbers agree closely with the theoretical curve.

Crossflow drag coefficient.- The variation with crossflow Mach number of the drag coefficient of a circular cylinder is presented in figure 15. Along with the present data, an accumulation of available cylinder data is included in this figure. Data from reference 11 have not been included since the tabulated pressure coefficients, when integrated, do not give overall drag coefficients equal to the values plotted in the same report. The data obtained by the crossflow method

appear to fair reasonably well within the scatter of existing low-supersonic Mach number data. It appears that the accuracy with which low Mach number data may be predicted from $M = 6.86$ data by use of the crossflow theory depends largely upon the fineness ratio of the test cylinder, the distance behind the nose of the cylinder that the pressure distribution is measured, and the angle of attack of the cylinder during the test. Since data obtained by the crossflow method agree with low-supersonic Mach number data, it appears that higher Mach number force coefficients may be predicted from $M = 6.86$ data. Included in figure 15 are the values of drag coefficient predicted by unmodified Newtonian flow, Grimminger's hypersonic approximation, and modified Newtonian flow for an infinite Mach number. From comparison of the present data at $M = 6.86$, and data from reference 10, it appears that the drag coefficient of a cylinder normal to the flow is relatively constant for Mach numbers above 4 and is adequately predicted by either Grimminger's hypersonic approximation or the modified Newtonian flow theories.

CONCLUSIONS

Analysis of experimental data obtained from tests made in the Langley 11-inch hypersonic tunnel on circular cylinders at a Mach number of 6.86 and a Reynolds number of 129,000 leads to the following conclusions:

1. The values of lift coefficient and drag coefficient of a circular cylinder at angles of attack of 14.9° through 90° agree favorably with the hypersonic approximation of Grimminger, Williams, and Young and with a simple modification of the Newtonian theory.

2. The pressure distribution around a circular cylinder given by the modified Newtonian theory agrees more favorably with experimental results than does that given by either Newtonian flow or the hypersonic approximation.

3. The calculated crossflow drag coefficients plotted as a function of crossflow Mach number were found to be in reasonable agreement with similar results obtained from other investigations at lower supersonic Mach numbers.

4. Comparison of the results of this investigation with the result obtained at lower supersonic Mach numbers indicates that the drag coefficient of a cylinder normal to the free-stream flow remains relatively

constant for Mach numbers above 4 and is adequately predicted by either the hypersonic approximation or the modified Newtonian theory.

Langley Aeronautical Laboratory,
     National Advisory Committee for Aeronautics,
          Langley Field, Va., January 6, 1954.

REFERENCES

1. Lord, Douglas R., and Ulmann, Edward F.: Pressure Measurements on an Ogive-Cylinder Body at Mach Number 4.04. NACA RM L51L20, 1952.

2. Grimminger, G., Williams, E. P., and Young, G. B. W.: Lift on Inclined Bodies of Revolution in Hypersonic Flow. Jour. Aero. Sci., vol. 17, no. 11, Nov. 1950, pp. 675-690.

3. Jones, Robert T.: Effects of Sweep-Back on Boundary Layer and Separation. NACA Rep. 884, 1947. (Supersedes NACA TN 1402.)

4. McLellan, Charles H., Williams, Thomas W., and Beckwith, Ivan E.: Investigation of the Flow Through a Single-Stage Two-Dimensional Nozzle in the Langley 11-Inch Hypersonic Tunnel. NACA TN 2223, 1950.

5. McLellan, Charles H., Bertram, Mitchel H., and Moore, John A.: An Investigation of Four Wings of Square Plan Form at a Mach Number of 6.86 in the Langley 11-Inch Hypersonic Tunnel. NACA RM L51D17, 1951.

6. McLellan, Charles H., Williams, Thomas W., and Bertram, Mitchel H.: Investigation of a Two-Step Nozzle in the Langley 11-Inch Hypersonic Tunnel. NACA TN 2171, 1950.

7. Clark, A. B. J., and Harris, Fred T. (With Appendix by R. E. Roberson): Free-Flight Air-Drag Measurement Techniques. NRL Rep. 3727, Naval Res. Lab., Sept. 6, 1950.

8. Charters, A. C., and Thomas, R. N.: The Aerodynamic Performance of Small Spheres From Subsonic to High Supersonic Velocities. Jour. Aero. Sci., vol. 12, no. 4, Oct. 1945, pp. 468-476.

9. Hodges, A. J.: The Drag Coefficient of Very High Velocity Spheres. Tech. Rep. No. T-656, Res. and Development Div., New Mexico School of Mines, 1949.

10. Gowen, Forrest E., and Perkins, Edward W.: Drag of Circular Cylinders for a Wide Range of Reynolds Numbers and Mach Numbers. NACA TN 2960, 1953.

11. Stanton, T. E.: On the Effect of Air Compression on Drag and Pressure Distribution in Cylinders of Infinite Aspect Ratio. R. & M. No. 1210, A.R.C., 1929.

12. Von Kármán, Th.: The Problem of Resistance in Compressible Fluids.
    R. Accad. d'Italia, Cl. Sci. Fis., Mat. e Nat., vol. XIII, 1935,
    pp. 210-265.

13. Welsh, Clement J.: The Drag of Finite-Length Cylinders Determined
    From Flight Tests at High Reynolds Numbers for a Mach Number
    Range From 0.5 to 1.3. NACA TN 2941, 1953.
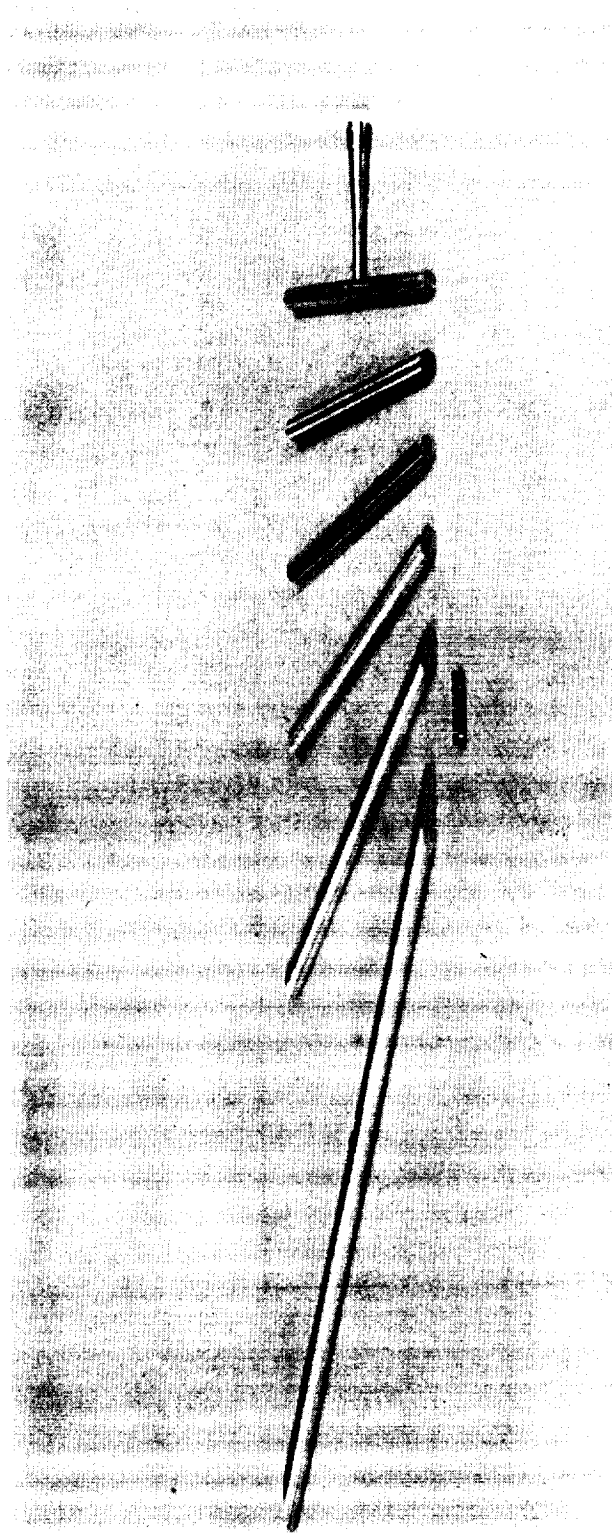
CONFIDENTIAL

L-80558

Figure 1.- Cylinder force models.
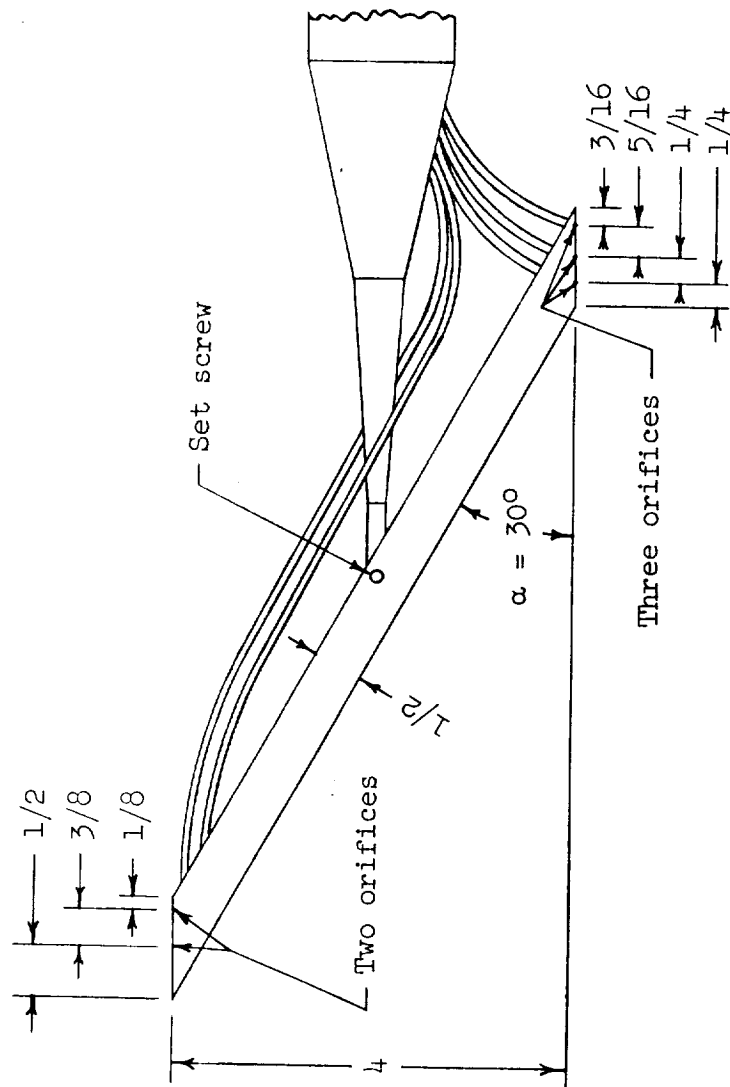
Figure 2.- Orifice installation on 30° force model. Dimensions are in inches.
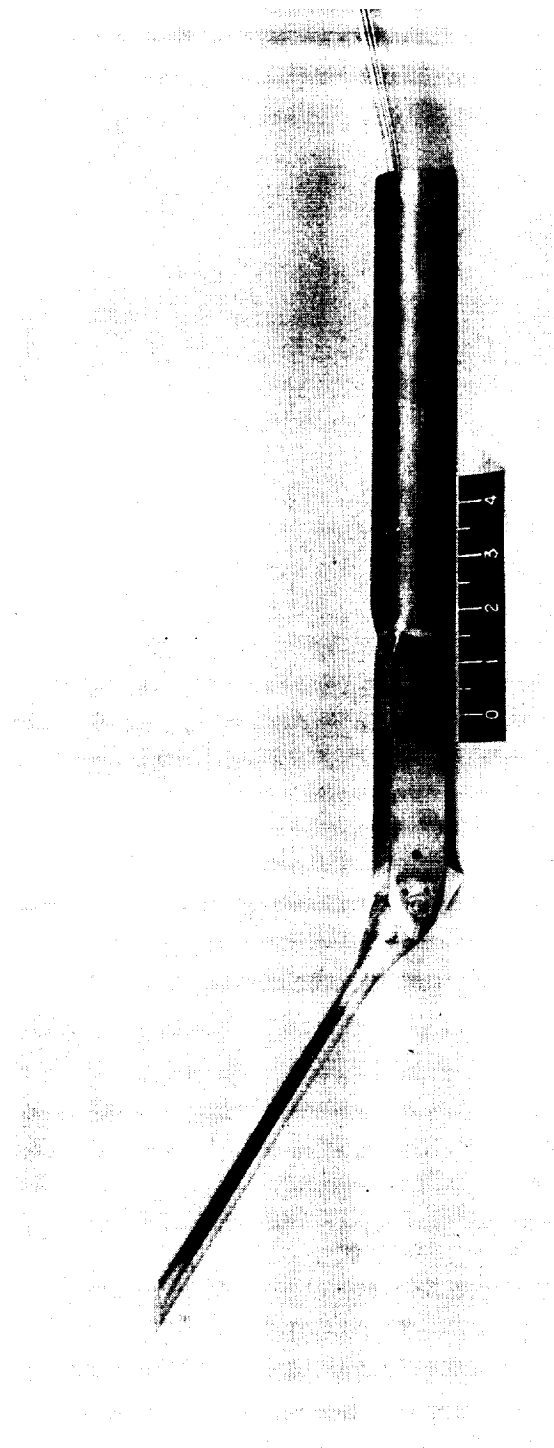
L-80773

Figure 3.- Cylinder pressure model.

α	X
15°	2 15/32
30°	1 1/2
45°	1 3/32
60°	29/32
75°	3/4
90°	5/8

Set screws

Six orifices evenly spaced radially, 60° apart

Set screw

9 1/8

4

2 5/8

7/8

1 5/8

1/2

X
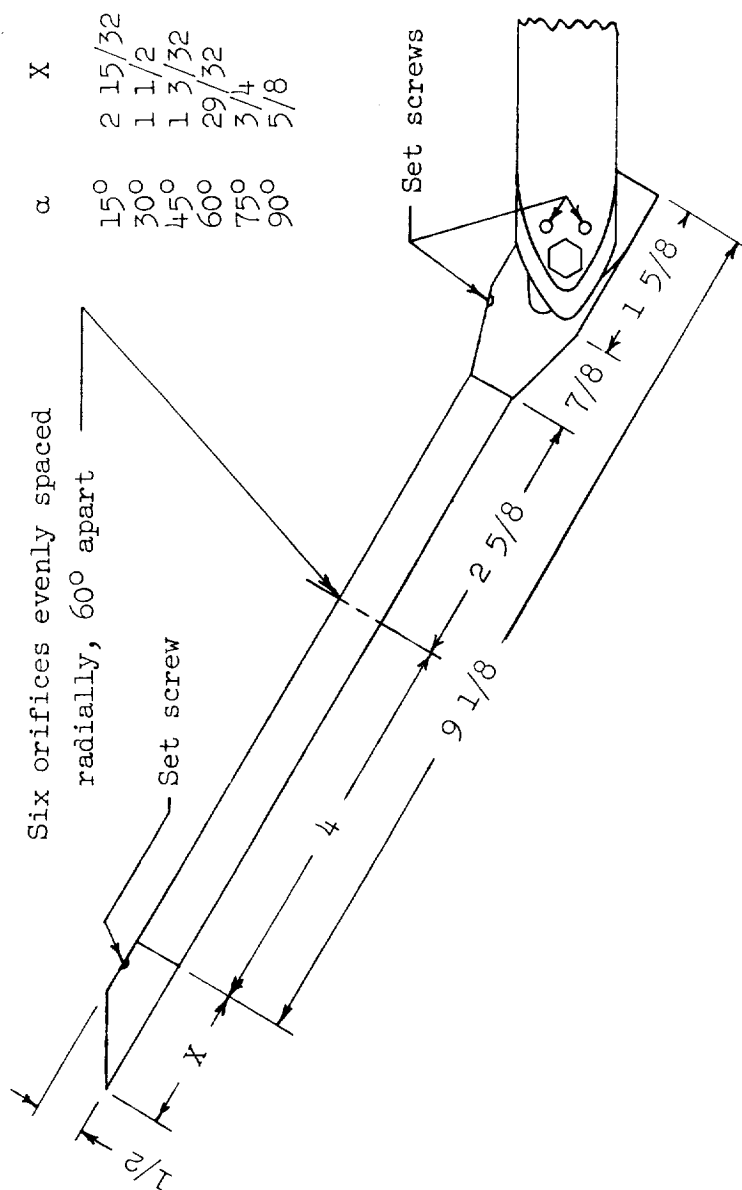
Figure 4.- Pressure model. Dimensions are in inches.
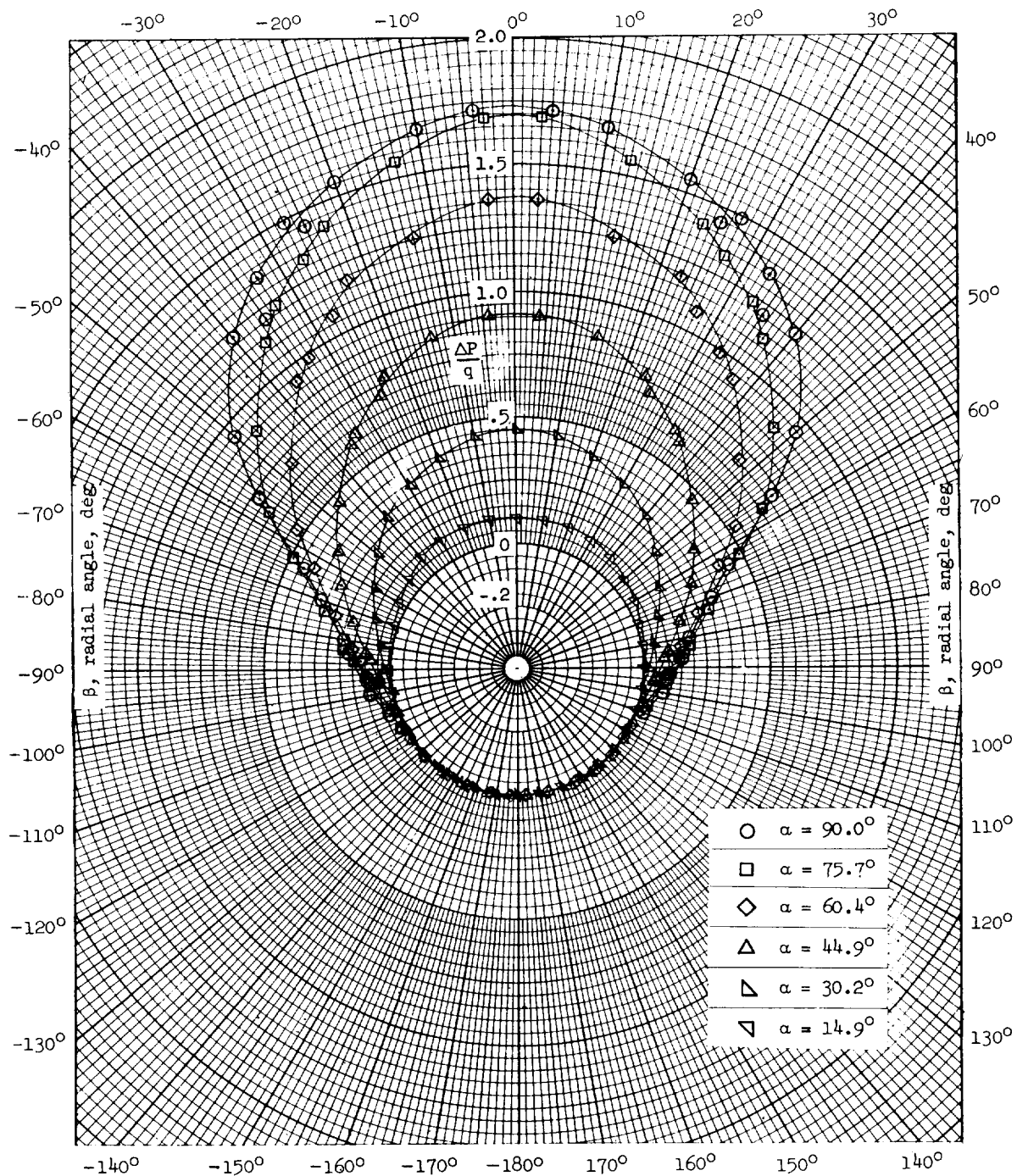
(a) Complete distribution.

Figure 5.- Variation with angle of attack of the pressure distribution around a circular cylinder at M = 6.86.
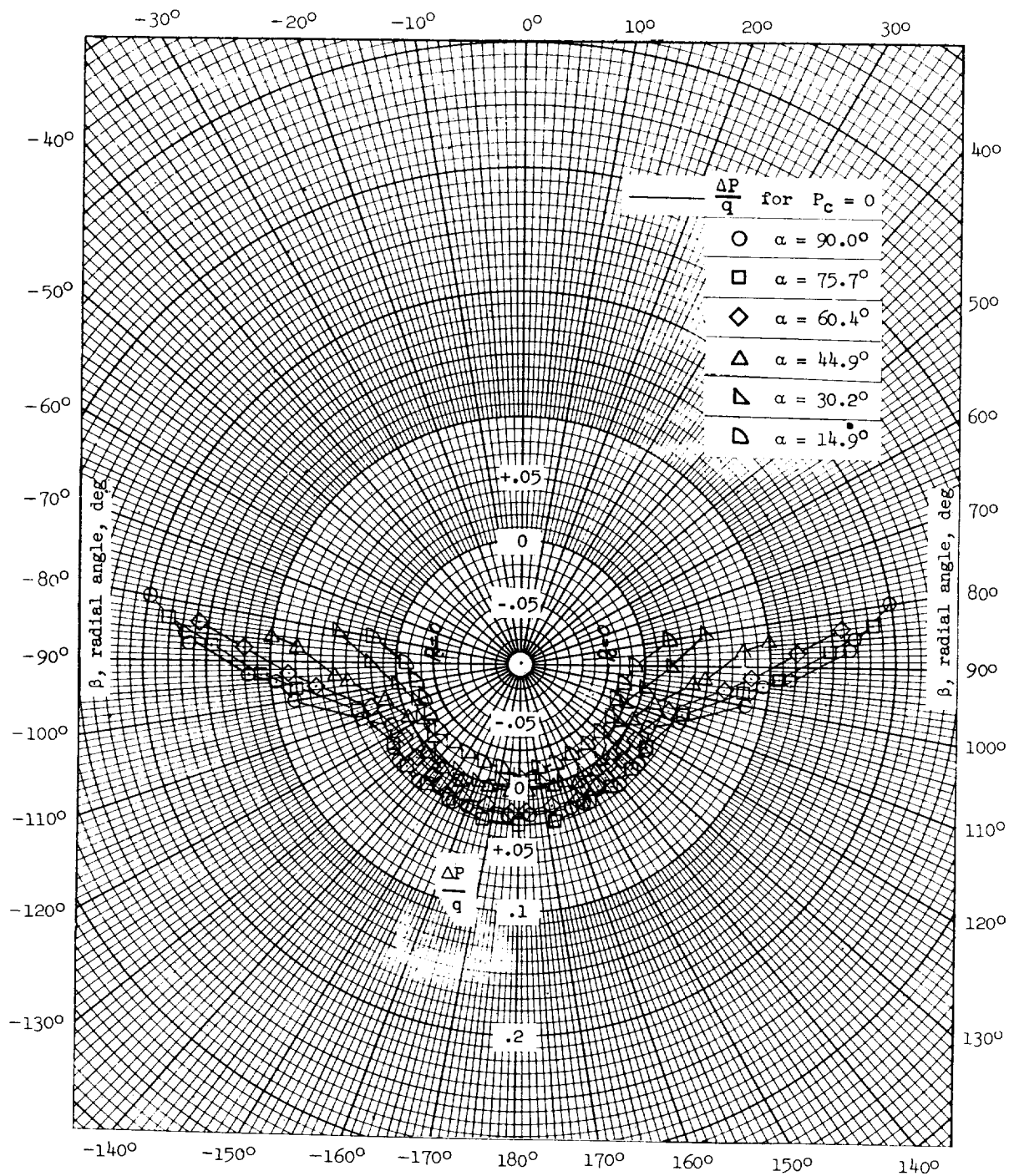
(b) Detailed view.

Figure 5.- Concluded.
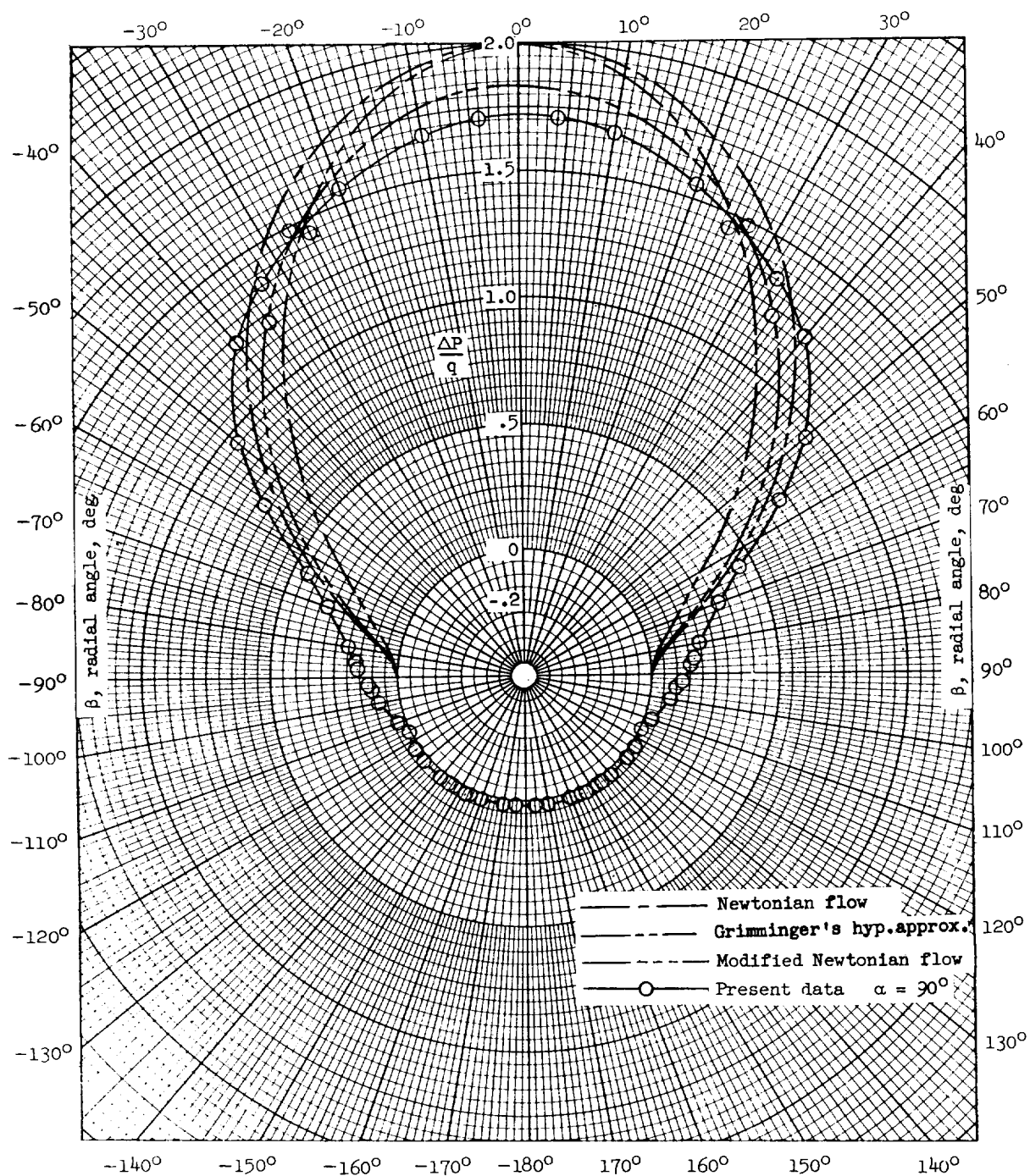
Figure 6.- Pressure distribution around a circular cylinder at α = 90°, M = 6.86.
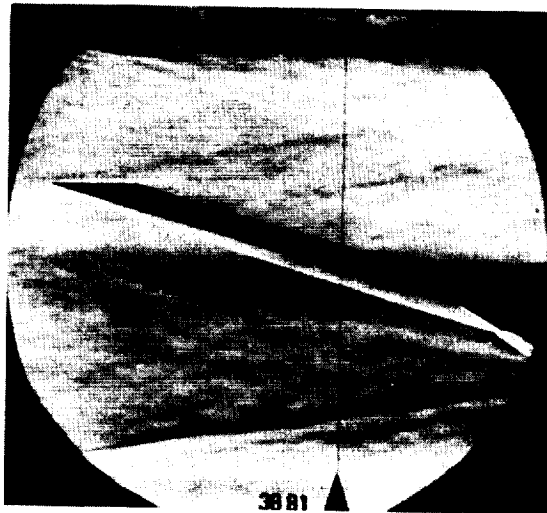
(a) Oblique tip, $\alpha = 15^{\circ}$.
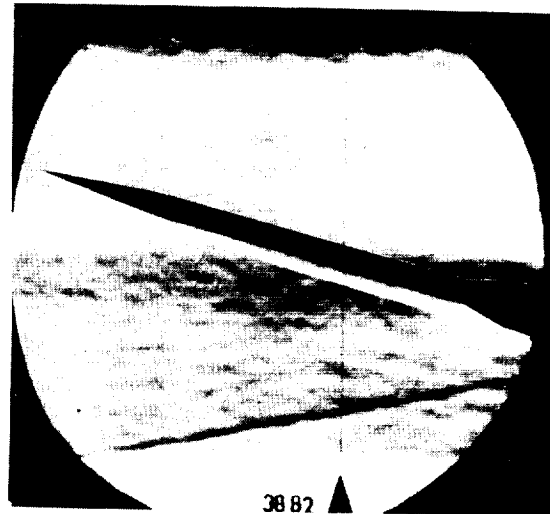
(b) 10° tip, $\alpha = 15^{\circ}$.
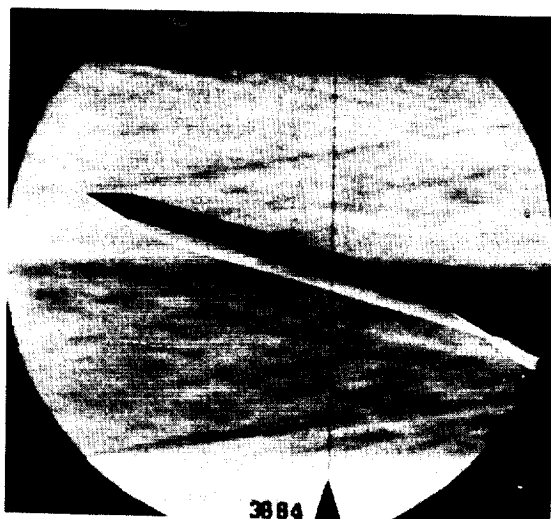
L-82073

(c) 30° tip, $\alpha = 15^{\circ}$.
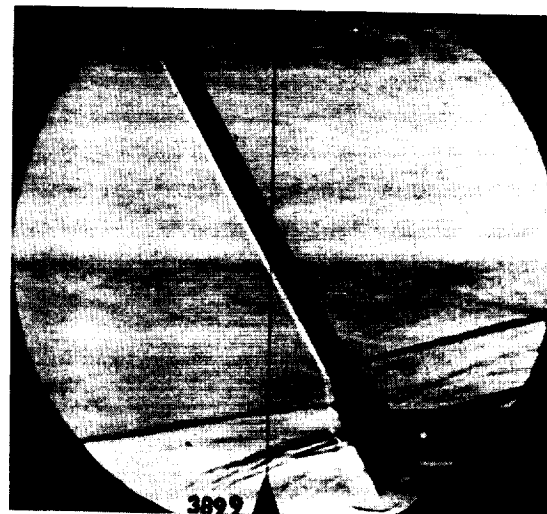
(d) Oblique tip, $\alpha = 60^{\circ}$.

Figure 7.- Schlieren photographs of cylinder pressure model, $M = 6.86$.
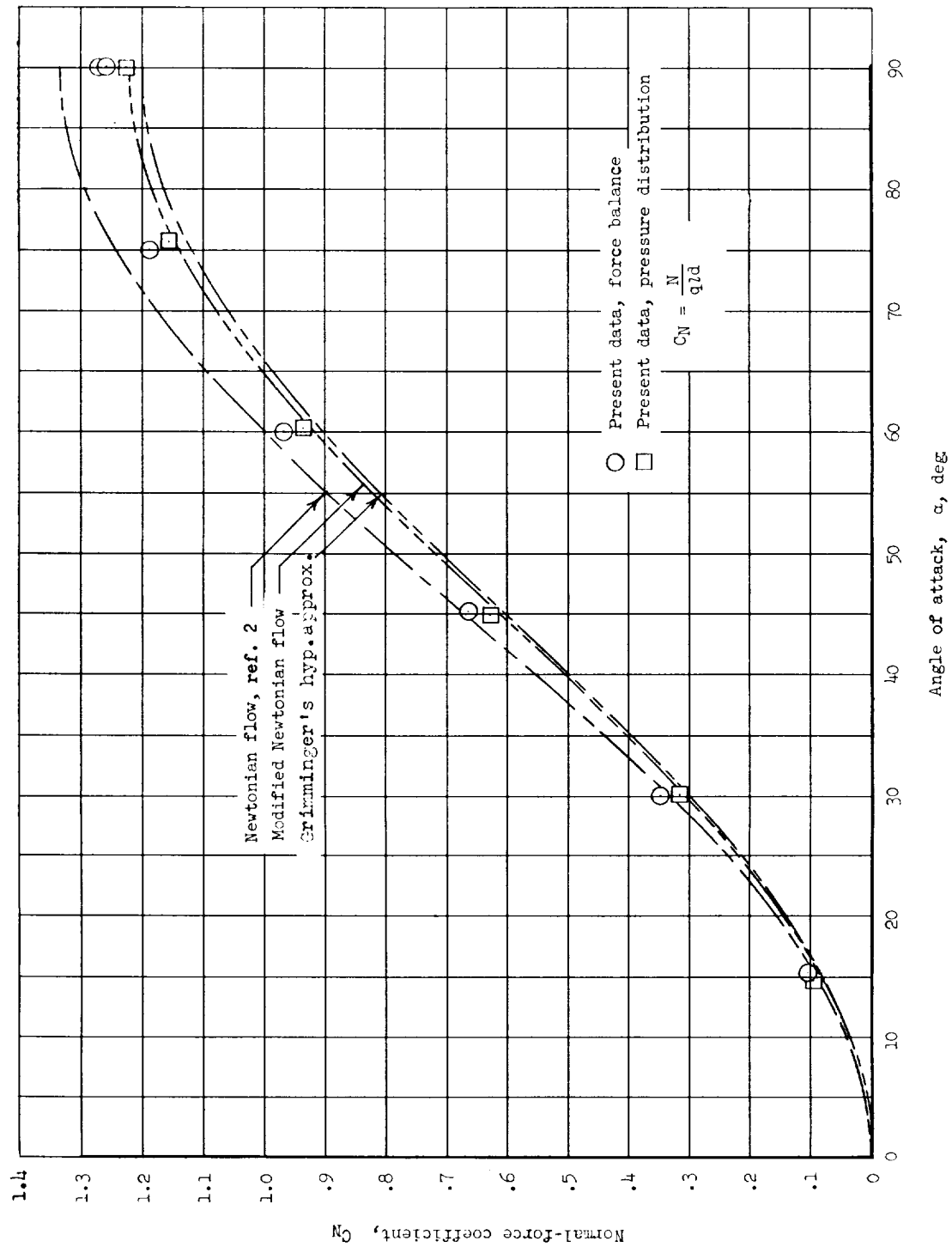
Figure 8.- Variation with angle of attack of the normal-force coefficient of a circular cylinder, M = 6.86.
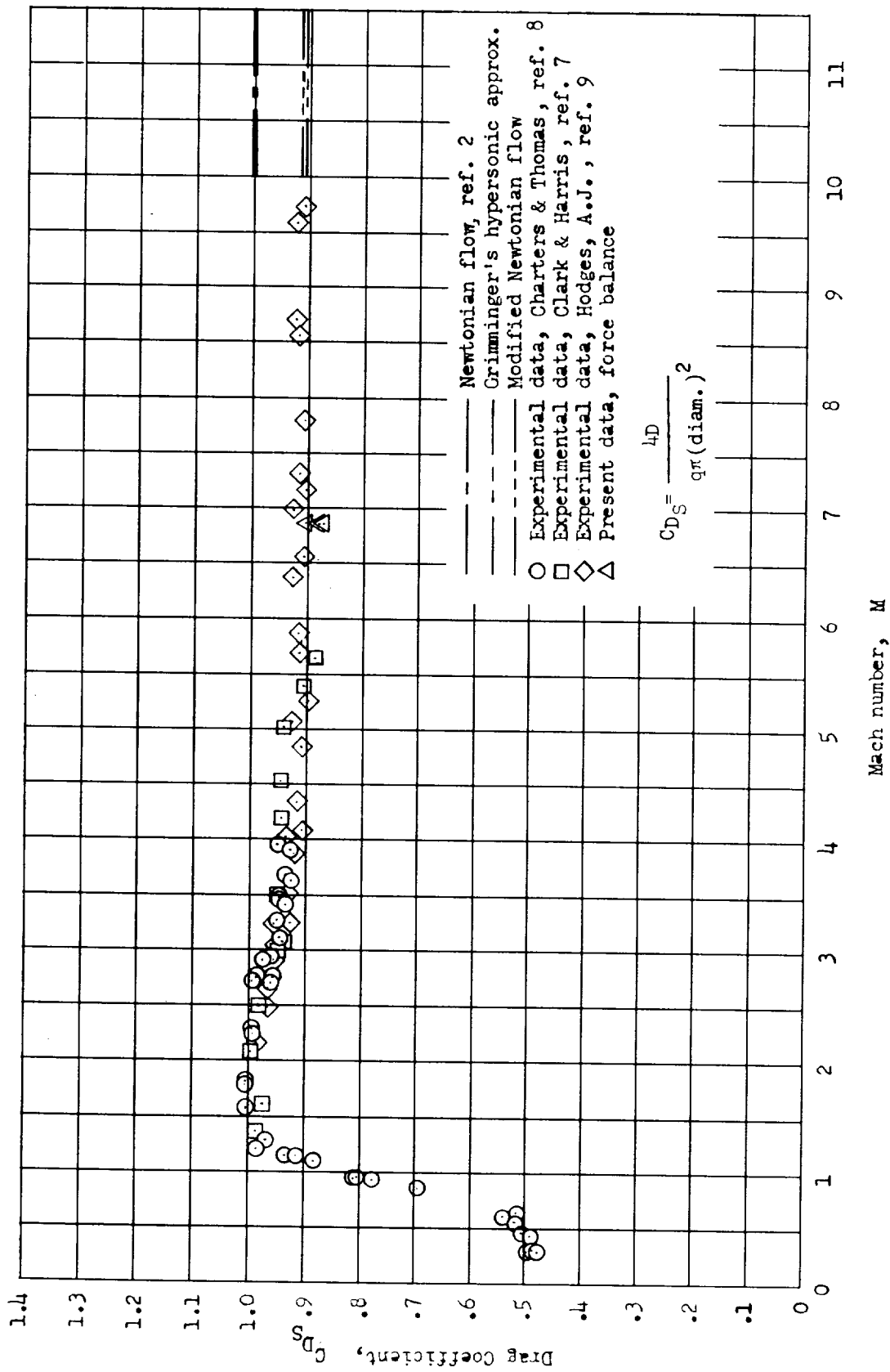
Figure 9.- Variation with Mach number of drag coefficient of a sphere.
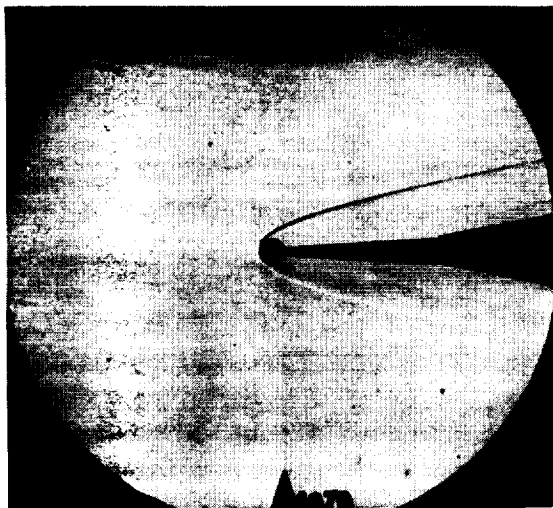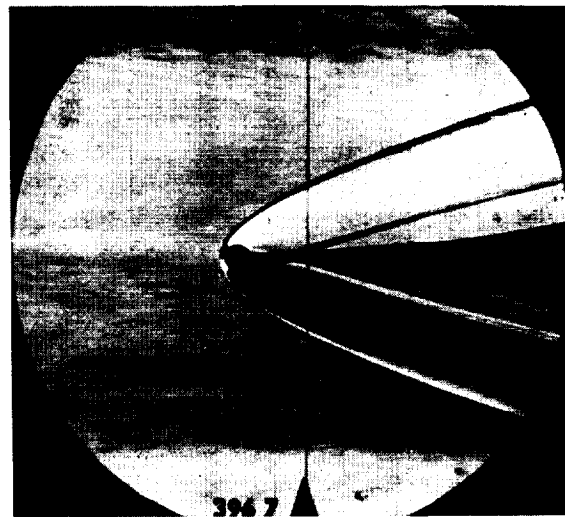
1/2-inch-diameter sphere   1/2-inch-diameter cylinder

L-82074

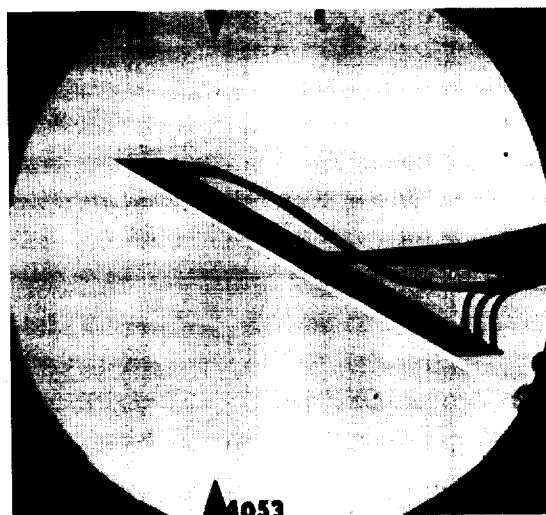Figure 10.- Schlieren photographs of 1/2-inch-diameter sphere and cylinder.
M = 6.86.
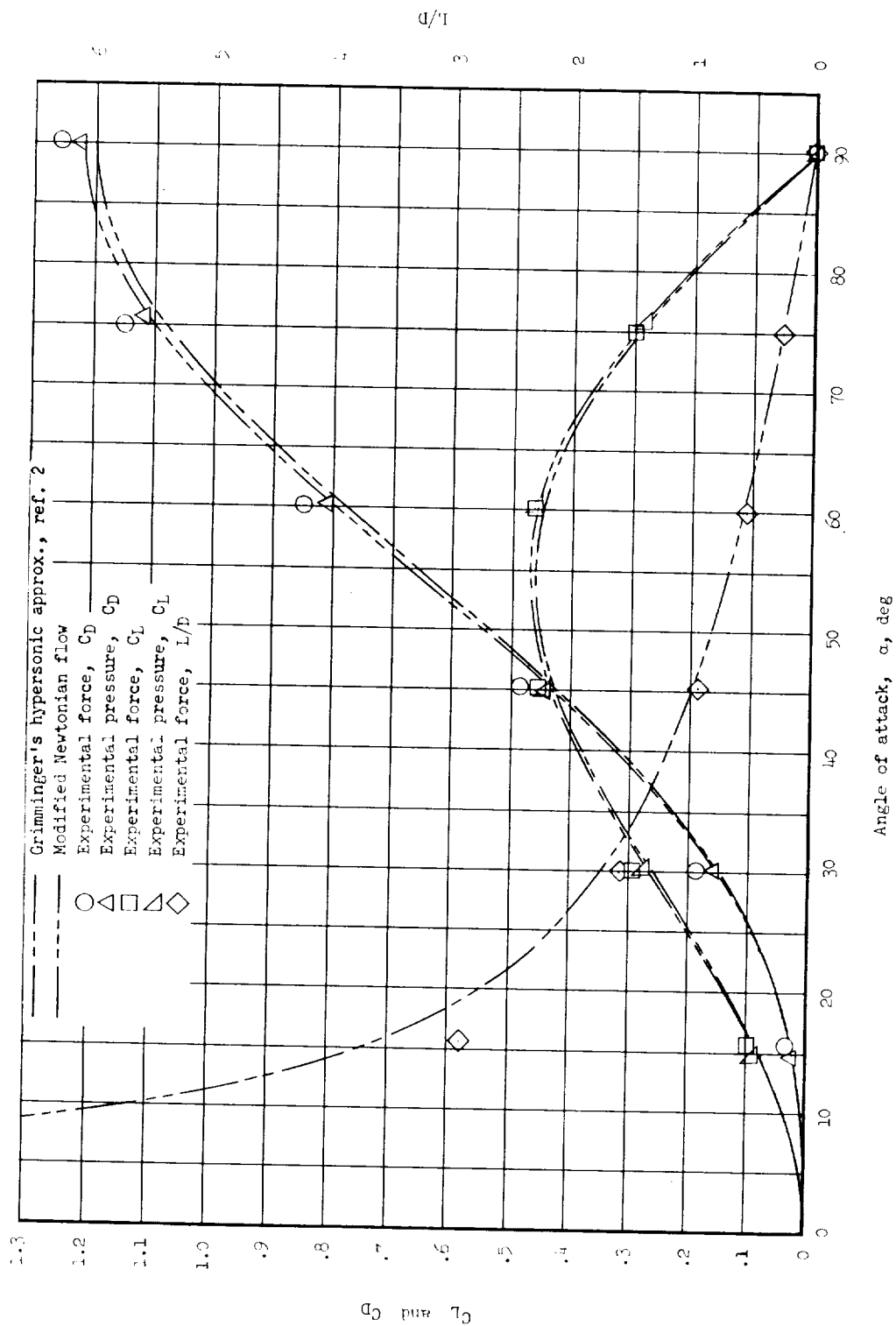
Figure 11.- Variation with angle of attack of the lift and drag coefficients of a circular cylinder. M = 6.86.

(a) $\alpha = 90°$.

(b) $\alpha = 60°$.
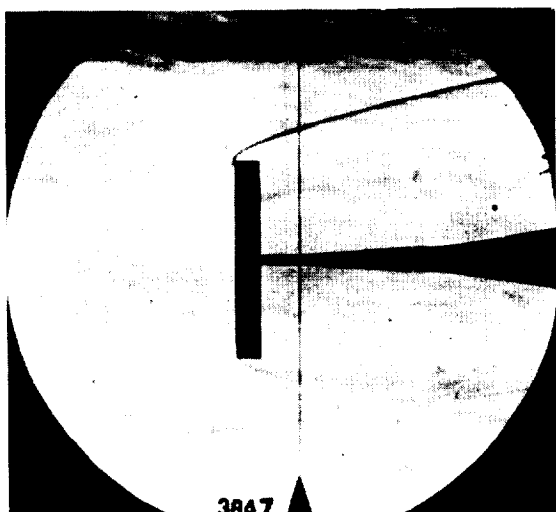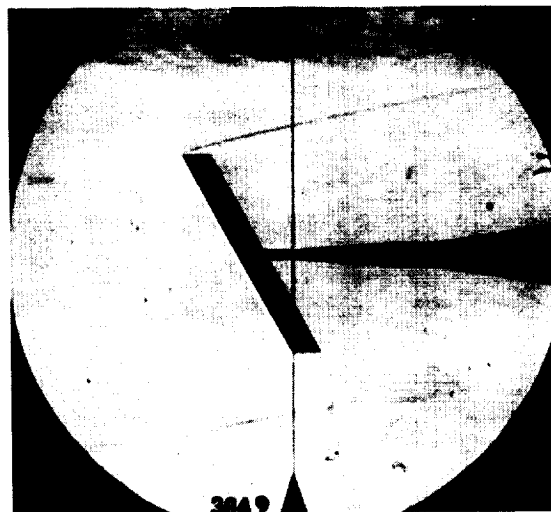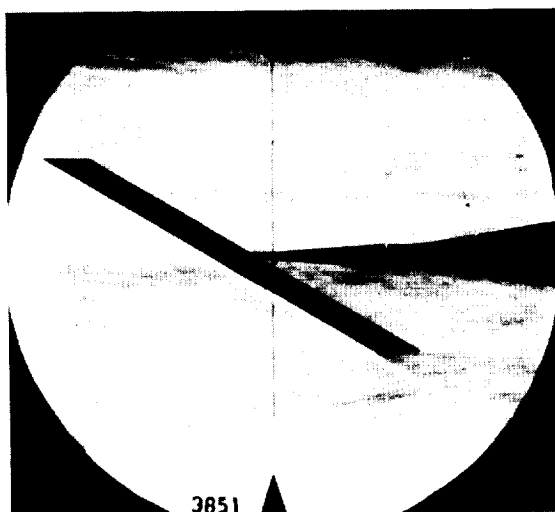
L-82075

(c) $\alpha = 30°$.

(d) $\alpha = 30°$, pressure
orifice installation.

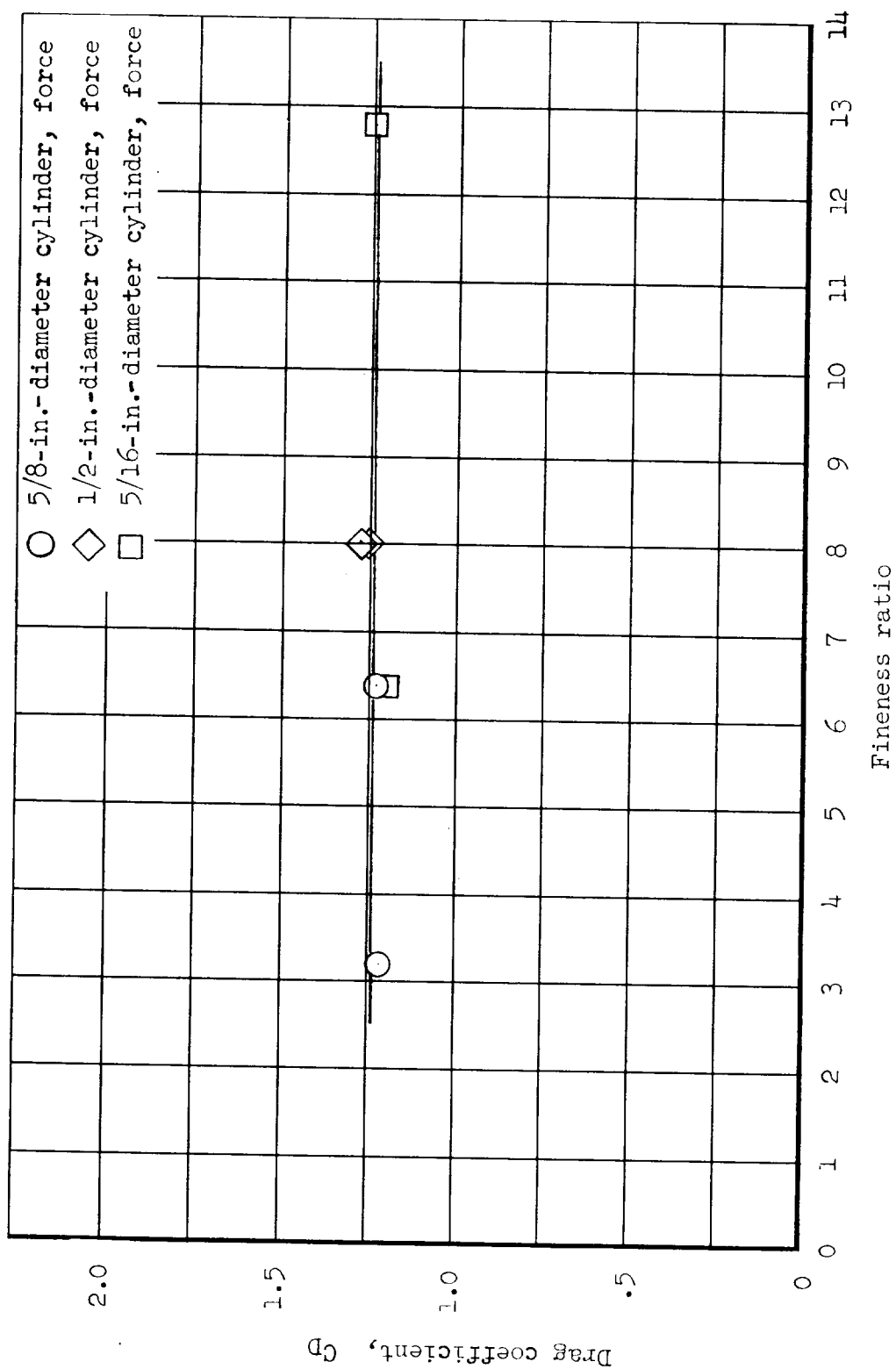Figure 12.- Schlieren photographs of cylinder force models. M = 6.86.

Figure 13.- Variation with fineness ratio of the drag coefficient of a circular cylinder normal to the flow. M = 6.86; Reynolds number = 257,000/inch.
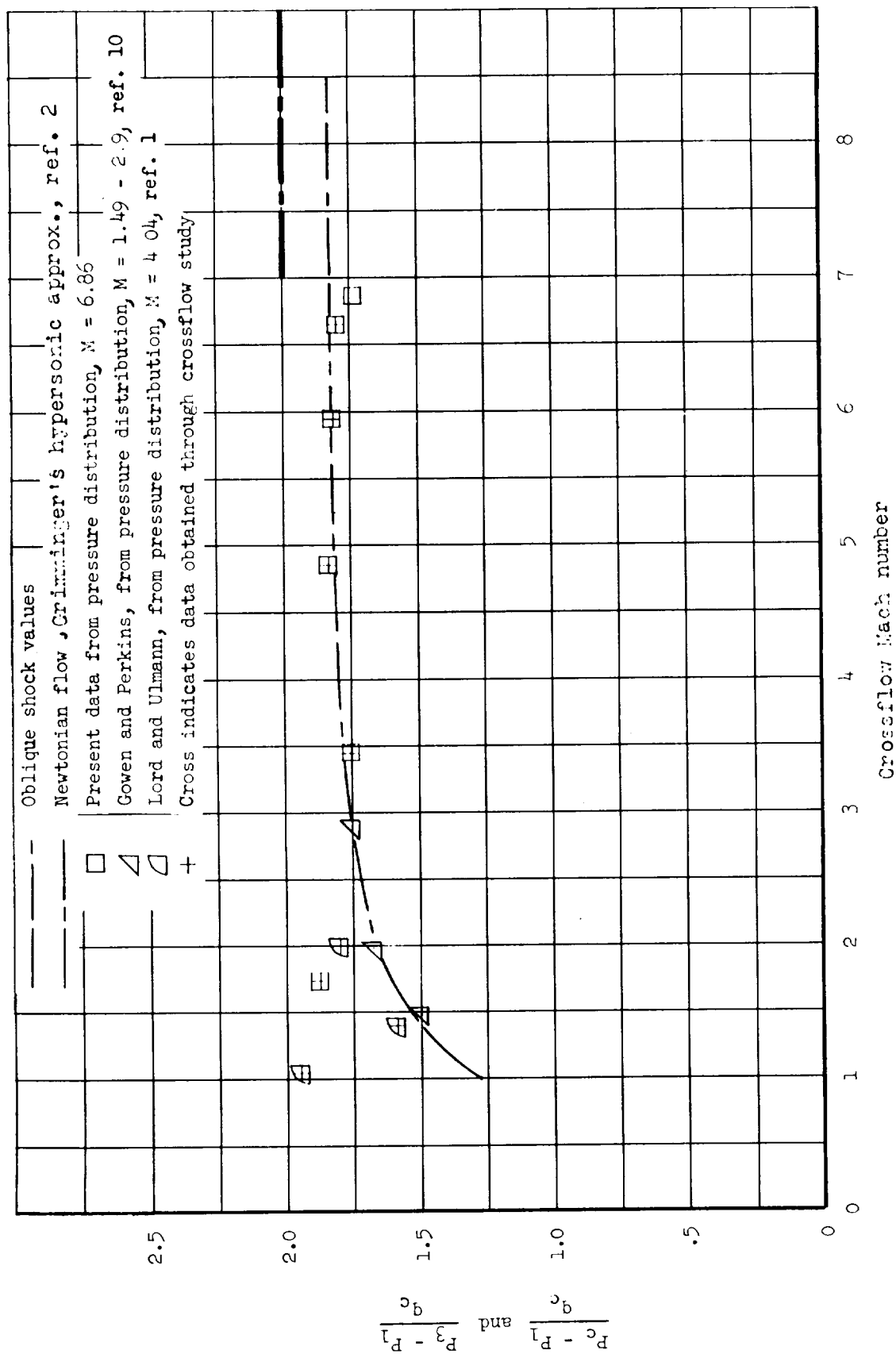
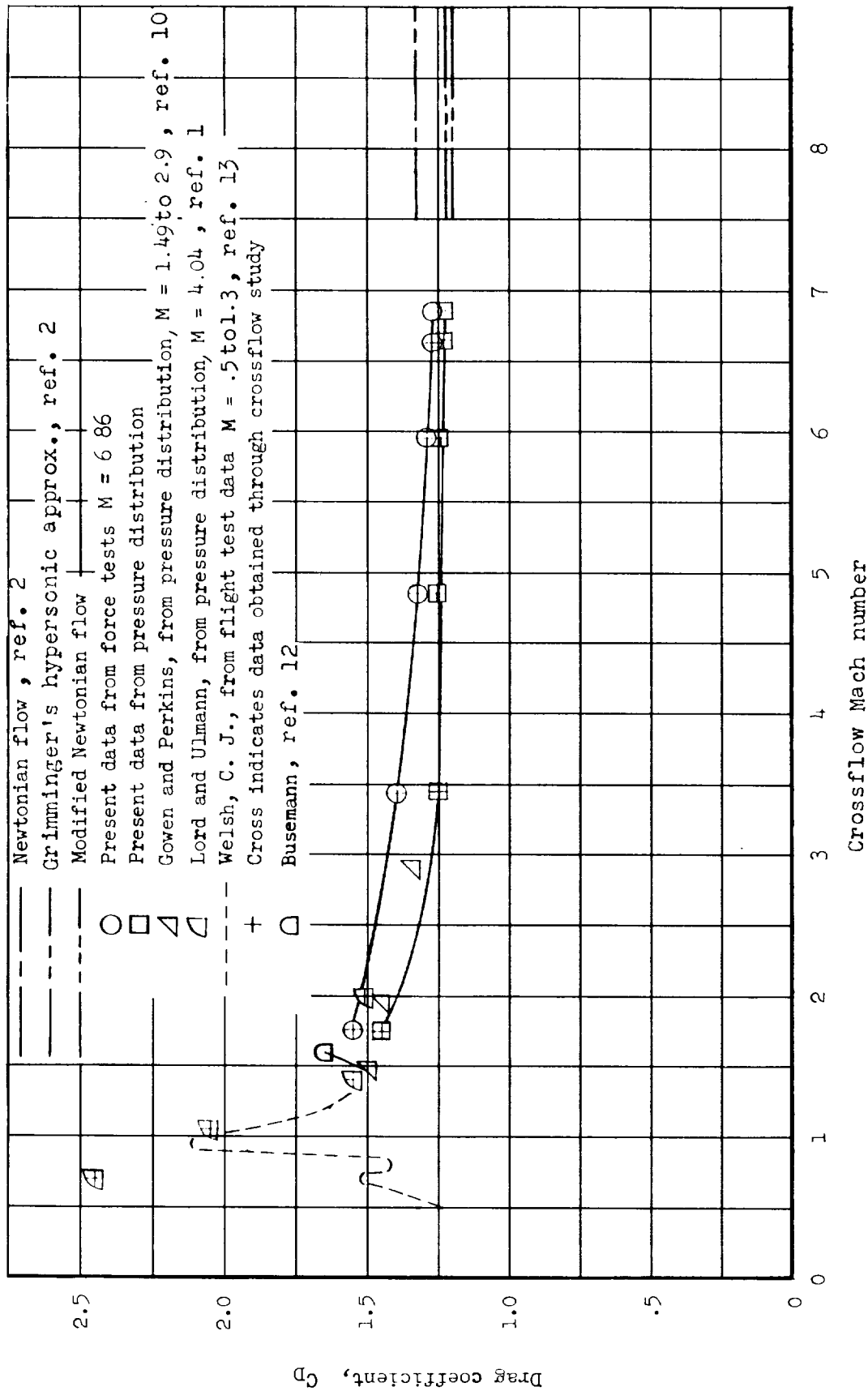Figure 14.- Variation with crossflow Mach number of the stagnation pressure coefficient of a circular cylinder.

Figure 15.- Variation with crossflow Mach number of the drag coefficient of a circular cylinder.